

^{13}C NMR Relaxation Rates in the Ionic Liquid 1-Methyl-3-nonylimidazolium Hexafluorophosphate

Jürgen H. Antony,[‡] Andreas Dölle, Dirk Mertens,[‡] Peter Wasserscheid,[‡]
W. Robert Carper,^{*,‡,†} and Phillip G. Wahlbeck[†]

Institut für Physikalische Chemie, Rheinisch-Westfälische Technische Hochschule Aachen, 52056 Aachen, Germany, and Department of Chemistry, Wichita State University, Wichita, Kansas 67260-0051

Received: April 7, 2005; In Final Form: June 2, 2005

A new method of obtaining molecular reorientational dynamics from ^{13}C spin–lattice relaxation data of aromatic carbons in viscous solutions is applied to ^{13}C relaxation data of the ionic liquid, 1-methyl-3-nonylimidazolium hexafluorophosphate ([MNIM]PF₆). Spin–lattice relaxation times (^{13}C) are used to determine pseudorotational correlation times for the [MNIM]PF₆ ionic liquid. Pseudorotational correlation times are used to calculate corrected maximum NOE factors from a combined isotropic dipolar and nuclear Overhauser effect (NOE) equation. These corrected maximum NOE factors are then used to determine the dipolar relaxation rate part of the total relaxation rate for each aromatic ^{13}C nucleus in the imidazolium ring. Rotational correlation times are compared with viscosity data and indicate several [MNIM]PF₆ phase changes over the temperature range from 282 to 362 K. Modifications of the Stokes–Einstein–Debye (SED) model are used to determine molecular radii for the 1-methyl-3-nonylimidazolium cation. The Hu–Zwanzig correction yields a cationic radius that compares favorably with a DFT gas-phase calculation, B3LYP/(6-311+G(2d,p)). Chemical shift anisotropy values, $\Delta\sigma$, are obtained for the ring and immediately adjacent methylene and methyl carbons in the imidazolium cation. The average $\Delta\sigma$ values for the imidazolium ring carbons are similar to those of pyrimidine in liquid crystal solutions.

Introduction

The development of new models and theories of the liquid state is of importance and general interest to workers in science and technology. In particular, these models and theories should provide a better understanding of molecular interactions relative to each other and their dynamic behavior in solution. Nuclear relaxation rates often provide valuable information concerning the dynamics and molecular interactions that occur in the liquid state.^{1–15} Use of nuclear spin–lattice relaxation rates to obtain information concerning reorientational dynamics is often restricted to the extreme narrowing region. In this region, the product of the resonance frequency and the rotational correlation time is less than unity. However, many ionic liquid systems of interest are viscous such that one is outside of the region of extreme narrowing and relaxation rates are frequency dependent. The rotational correlation equations that describe the frequency-dependent region are considerably more complex and analysis is somewhat more difficult.

In a recent ^{13}C NMR relaxation study¹⁶ of the viscous ionic liquid 1-butyl-3-methylimidazolium hexafluorophosphate ([BMIM]PF₆), a new method was used to separate dipolar and chemical shift anisotropy for aromatic carbons. This report contains the application of this method to the ionic liquid, 1-methyl-3-nonylimidazolium hexafluorophosphate ([MNIM]PF₆). The ionic liquid [MNIM]PF₆ is similar to [BMIM]PF₆ with the exception that there is a considerably longer (nonyl) side chain attached to the imidazolium ring. This allows one to observe the effects

of a long side chain on the ^{13}C rotational microdynamics of both the side chain and the imidazolium ring.

The models and correlation equations that are useful to the investigator include those developed by Abragam and others,^{1–7} which describe rotational molecular motion and its relationship with intramolecular events. Dipolar relaxation can be directly related to rotational motion with the use of spherical harmonic functions. Solution of the resulting autocorrelation functions produces spectral density functions, assuming exponential decay. The spectral density equations are correlation time dependent at a set frequency^{1–3} and describe spin–lattice (longitudinal: $R_1 = 1/T_1$) and spin–spin (transverse: $R_2 = 1/T_2$) relaxation mechanisms that include dipole–dipole, chemical shift anisotropy, spin rotation, scalar relaxation, and quadrupole relaxation.

It should be emphasized that the model of intramolecular rotation is isotropic in nature. In the case of anisotropic motion, these equations do not hold, and must be modified to account for different motional characteristics. For example, the correlation function representing relaxation caused by random translational diffusion is not a single exponential. Another limitation is the possibility of a distribution of correlation times caused by internal motion in a macromolecule. Despite these potential limitations, evidence reported previously^{8–12,14,15} indicates that the isotropic model can be used successfully to study a significant number of molecular and ionic systems in solution.

A relatively new method is used herein to determine ^{13}C NMR dipolar and chemical shift anisotropy relaxation rates of the highly viscous ionic liquid 1-methyl-3-nonylimidazolium hexafluorophosphate ([MNIM]PF₆). The classical dipolar relaxation model and NOE factors are used to study the imidazolium ring and its attached aliphatic groups in the 1-methyl-3-nonylimidazolium hexafluorophosphate ([MNIM]PF₆) ionic liquid. The

* Address correspondence to this author. E-mail: bob.carper@wichita.edu.

[‡] Rheinisch-Westfälische Technische Hochschule Aachen.

[†] Wichita State University.

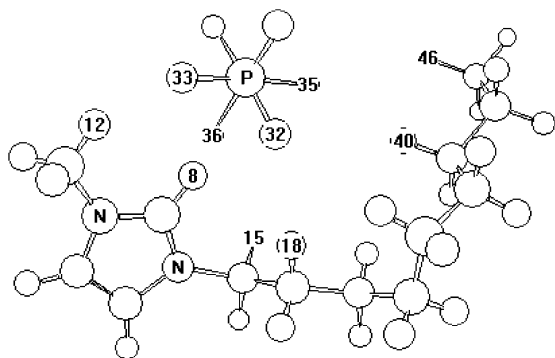


Figure 1. DFT (gas phase) molecular structure of [MNIM]PF₆ (B3LYP/6-311+G(2d,p)). Hydrogen bonds include the following: F33–H12 = 2.380 Å; F33–H8 = 2.160 Å; F36–H8 = 2.486 Å; F36–H15 = 2.375 Å; F32–H8 = 2.002 Å, F32–H15 = 2.789 Å, F32–H18 = 2.498 Å, F32–H40 = 2.773 Å, F35–H40 = 2.748 Å and F35–H46 = 2.659 Å.

theoretical gas-phase structure of 1-methyl-3-nonylimidazolium hexafluorophosphate ([MNIM]PF₆) is shown in Figure 1. The hydrogen bonds between the imidazolium C2 hydrogen and PF₆[−] in Figure 1 are similar to those reported elsewhere for the ionic liquid [BMIM]PF₆.¹⁷

Experimental Section

A modification of the method described by Fuller et al. was used for the synthesis of 1-ethyl-3-methylimidazolium hexafluorophosphate.¹⁸ In this modified synthesis, 48.9 g (0.2 mol) of 1-methyl-3-nonylimidazolium chloride ([MNIM]Cl) is dissolved in 100 mL of water and cooled to 5 °C. At this point, 29.2 g (0.2 mol) of 60% aqueous HPF₆ is added dropwise. The product precipitates as a slightly yellow liquid in a second liquid layer. After phase separation the ionic liquid layer is extracted five times with 100 mL of water to remove all traces of HCl. The crude, slightly yellow ionic liquid is dried overnight at 60 °C under high vacuum to remove all traces of water. This is followed by column chromatography, as the ionic liquid is dissolved in a 2-fold volume of methylene chloride and Silica 60 is used as the column material. After this purification step the ionic liquid is isolated in 80% overall yield as a colorless liquid after removal of the CH₂Cl₂ in vacuo.

NMR Relaxation Measurements

The ¹³C NMR relaxation data were measured on a Bruker AM 250 spectrometer (*B*₀ = 5.875 T, *v*₀(¹³C) = 62.89 MHz, *v*₀(¹H) = 250.13 MHz, lock on ²H in a deuterated solvent in a 10 mm NMR tube surrounding an inner NMR tube of 7.5-mm diameter containing [MNIM]PF₆). The spin–lattice relaxation times were measured by using the inversion–recovery pulse sequence and calculated from the ¹H-broadband-decoupled ¹³C spectra by a single-exponential fit (*R*² = 0.999) with no evidence of double exponential behavior. The relaxation data were extracted from the signal heights. The measurements of the spin–lattice relaxation times were repeated at least five times, those for the NOE factors 10 times, and then the average values were used further. The error in the temperature was estimated to be ±1 K. Chemical shift values were determined with COSY and HETCOR methods.

Methodology

¹³C NMR Relaxation Studies. The relaxation of ¹³C in medium-sized molecules at moderate magnetic fields is usually caused by dipolar interactions with directly bonded protons.

When the relaxation times are measured under ¹H decoupling conditions, the cross-relaxation term vanishes, and the intramolecular dipolar longitudinal (spin–lattice) relaxation rate (*R*₁^{DD} = 1/*T*₁^{DD})_{*i*} for the relaxation of ¹³C nucleus *i* by *N*_H protons *j* is connected to the molecular reorientations by:^{1–6}

$$\left[\frac{1}{T_1^{DD}} \right]_i = [1/20]N_H[2\pi D_{ij}]^2[J(\omega_C - \omega_H) + 3J(\omega_C) + 6J(\omega_C + \omega_H)] \quad (1)$$

where the dipolar coupling constant is *D*_{*ij*} = (μ₀/4π)γ_Cγ_H(ħ/2π)*r*_{*ij*}^{−3}, μ₀ is the permeability of the vacuum, γ_C and γ_H are the magnetogyric ratios of the ¹³C and ¹H nuclei, respectively, and *r*_{*ij*} is the length of the internuclear vector between *i* and *j* (C–H = 1.09 Å). *J*(ω) are the spectral densities with ω_C and ω_H the resonance frequencies of the ¹³C and ¹H nuclei, respectively.

Nuclear Overhauser Effect. The nuclear Overhauser (NOE) factor η_{*i*} of carbon atom *i* relaxed by *N*_H protons *j* is given by:^{1–6,13}

$$\eta_i = \gamma_H \sum \sigma_{ij} / [\gamma_C \sum (\rho_{ij} + \rho_i^*)] \quad (2)$$

where Σ includes from *j* = 1 to *N*_H, σ_{*ij*} is the cross-relaxation rate, ρ_{*ij*} is the dipolar relaxation rate, and ρ_{*i*}^{*} is the leakage term that represents the contribution of all other relaxation mechanisms to the relaxation of a ¹³C nucleus *i*, thus reducing the NOE factor. Usually, intermolecular dipolar contributions can be neglected for ¹³C nuclei with directly bonded protons. Under ¹H decoupling conditions, the sum of ρ_{*ij*} over all *N*_H interacting protons gives the dipolar spin lattice relaxation rate (*R*₁^{DD} = *R*₁^{Dipolar} = 1/*T*₁^{Dipolar})_{*i*}. The relaxation of ¹³C exclusively via intramolecular dipolar interaction implies a leakage term ρ_{*i*}^{*} = 0. Thus the NOE factor reaches its maximum value and depends only on reorientational molecular dynamics:^{1–6,13}

$$\eta_{i,max} = \gamma_H [6J(\omega_C + \omega_H) - J(\omega_C - \omega_H)] / \gamma_C [J(\omega_C - \omega_H) + 3J(\omega_C) + 6J(\omega_C + \omega_H)] \quad (3)$$

Spectral Densities. Assuming isotropic tumbling, the spectral densities can be connected to the effective correlation times, τ_c, for reorientation of the corresponding internuclear ¹³C–¹H vectors by:

$$J(\omega) = 2\tau_c / [1 + (\omega\tau_c)^2] \quad (4)$$

In theory τ_c is the time required for a molecule (i.e., vector connecting the interacting nuclei) to rotate through an angle of one radian; however, in fact, the correlation time is the integral with respect to time from 0 to ∞ of the normalized autocorrelation function^{2,6} and is actually τ₂, the time constant for the exponential decay of the second-rank Legendre polynomial P₂. In the extreme narrowing case (low viscosity solutions—unlike ionic liquids) the product of ωτ_c is much less than unity and *J*(ω) = 2τ_c.

Chemical Shift Anisotropy (CSA). Aromatic ¹³C nuclei relax even in moderate magnetic fields partially via the chemical-shift anisotropy (CSA) mechanism. The corresponding longitudinal relaxation rate of the ¹³C nucleus *i* is given by:^{1–6}

$$R_1^{CSA} = [1/15]\gamma_C^2 H_0^2 (\Delta\sigma_i)^2 [1 + (\eta_{csa}^2/3)]J(\omega_C) \quad (5)$$

with the magnetic field strength *H*₀, the chemical-shift anisotropy Δσ for an axially symmetric chemical shift tensor, and the

asymmetry parameter, η_{CSA} . The $[1 + \eta_{\text{CSA}}^2/3]$ term usually represents a correction factor of less than 5% and is therefore ignored.

Solution of the Combined Dipolar and NOE Equations.

In the case of ring (aromatic) carbons, it is assumed that dipolar relaxation and chemical shift anisotropy make up the overall relaxation rate:

$$R_1^{\text{total}} = R_1^{\text{Dipolar}} + R_1^{\text{CSA}} \quad (6)$$

The dipolar (R_1^{Dipolar}) and chemical shift anisotropy (R_1^{CSA}) spin–lattice relaxation rates for aromatic carbons may be obtained as follows: (1) The experimental T_1 's are assumed to be completely dipolar and eq 1 is solved for a pseudorotational correlation time as follows:

$$\tau_c = [10/T_1 N_H (2\pi D_{ij})^2] [1/[1 + (\omega_C - \omega_H)^2 \tau_c^2] + (3/[1 + \omega_C^2 \tau_c^2]) + (6/[1 + (\omega_C + \omega_H)^2 \tau_c^2])] \quad (7)$$

Values of τ_c were calculated by successive approximations by setting τ_c on the right-hand side of eq 7 equal to the previously calculated value. The initial value of τ_c was set at 0.01 ns. A constant value of τ_c was obtained after approximately 5 iterations; however, the value after 40 iterations was utilized.

(2) Equations 1 and 3 are combined to form eq 8. The experimental T_1 's and the pseudorotational correlation times from eq 7 were used in eq 8 to calculate η_{max} . If these values of η_{max} were greater than 1.99, η_{max} was set equal to 1.99.

$$\eta_{\text{max}} = N_H [T_1^{DD}/20] (\gamma_H/\gamma_C) (2D_{ij})^2 [6J_+ - J_-] \quad (8)$$

where $J_+ = [2\tau_c/[1 + (\omega_C + \omega_H)^2 \tau_c^2]]$ and $J_- = [2\tau_c/[1 + (\omega_C - \omega_H)^2 \tau_c^2]]$.

The corrected ring carbon R_1^{Dipolar} is then calculated by using the experimental T_1 's as follows:

$$R_1^{\text{Dipolar}} = (\text{NOE}/\text{NOE}_{\text{max}})/T_1^{\text{total}} \quad (9)$$

The result obtained from eq 9 is then used to solve eq 1 to determine a corrected rotational correlation time (τ_c) for each aromatic carbon. It is then possible to do a repeating set of calculations using the previously established values for R_1^{Dipolar} to generate new values for τ_c , η_{max} and new R_1^{Dipolar} . After three cycles, the values of τ_c are reasonably well established.

Finally, the aromatic carbon chemical shift anisotropy (R_1^{CSA}) spin–lattice relaxation rates are determined from eq 6. Equation 5 is then used to calculate the chemical shift anisotropy ($\Delta\sigma$) for an axially symmetric chemical-shift tensor.

Results and Discussion

Basic Assumptions. The basic assumption in this analysis is that the maximum value of the ^{13}C NOE in eq 3 is determined by the dipolar rotational correlation time obtained from the measured relaxation rate. As outlined in the previous sections, eq 1 is solved for the rotational correlation time, assuming that the measured ^{13}C relaxation rate is completely dipolar. This rotational correlation time is then used with eq 7 to determine a maximum NOE value (≤ 1.988 for ^{13}C). This maximum NOE value is then compared with the measured NOE value and eq 8 is used to generate a new (corrected) value of the dipolar relaxation rate. This new value of the ^{13}C dipolar relaxation rate is used to solve eq 1 for the final (corrected) rotational correlation time. Finally, eq 6 is used to determine the amount

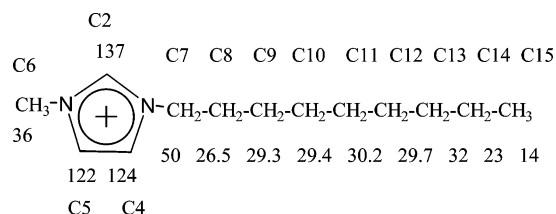


Figure 2. Chemical shift values (^{13}C , ppm) and carbon positions for the 1-methyl-3-nonylimidazolium cation in the [MNIM]PF₆ ionic liquid.

of the experimentally determined ^{13}C relaxation rate that is due to chemical shift anisotropy.

Sources of Error. As indicated previously,¹⁶ there are questions of biexponential behavior and the use of an isotropic model to describe anisotropic motion. For example, eq 5 (CSA) assumes isotropic motion such that geometric (principal components of the shielding tensor) and dynamic components can be separated. In particular, even small rotational anisotropies may have a major effect on eq 5.

First of all, there appear to be few (if any) examples of biexponential behavior in the literature as far as viscous solutions of this type (ionic liquids and molten salts) are concerned. Despite its inherent assumptions, the isotropic model has proved to be reasonably successful in describing a wide range of viscous solutions and providing useful physical information concerning such systems.^{8,15,16}

However, there are other problems that are easily detected including scalar relaxation and chemical exchange.⁸ In this study, scalar relaxation will not be a factor as it arises only when (a) the Larmor frequencies are similar (carbon bonded to bromine) or when (b) a slowly relaxing nucleus is bonded to a fast relaxing nucleus (carbon bonded to aluminum). Another relaxation mechanism that can contribute to line broadening is that of chemical exchange. Chemical exchange is generally present when the observed NMR peak broadens out with increasing temperature and then separates into two or more peaks when the exchange rate between species is faster than the NMR time scale. Temperature studies of [BMIM]PF₆ have failed to indicate any of the above relaxation mechanisms in this ionic liquid ([MNIM]PF₆).

Finally, there is the question of molecular mobility when using the isotropic model. A detailed analysis of this system with use of isotropic and related models provides a reasonable description of molecular mobility.¹⁵ This analysis was recently supported by a molecular dynamics study of [BMIM]PF₆.¹⁹ In a theoretical study²⁰ of homonuclear NOE's as probes of molecular mobility, it was concluded that in general, NOE's are insensitive to internal mobility and depend solely on overall molecular mobility. The extension of this conclusion to heteronuclear systems is supported to a limited extent by the correlation between diffusion coefficients and ^{13}C relaxation rates in viscous solutions.^{10–12}

Chemical Shifts and Relaxation Times. Figure 2 contains the ^{13}C chemical shifts of the [MNIM] cation relative to TMS and Figure 3 is a plot of the ^{13}C correlation times (ps) vs temperature (K). Figure 3 contains the ^{13}C total spin relaxation times for imidazolium and selected side chain carbons in the [MNIM]PF₆ ionic liquid. The imidazolium ring carbons, the methyl and methylene carbons attached directly to the imidazolium ring, have a minimum in the region of 30–40 °C. The terminal methyl and all of the remaining methylene carbons have minima at temperatures less than –10 °C. Similar results were obtained for the [BMIM]PF₆ ionic liquid.

Corrected Maximum Noe Factors. The corrections to the maximum noe factors in the [MNIM]PF₆ ionic liquid are quite

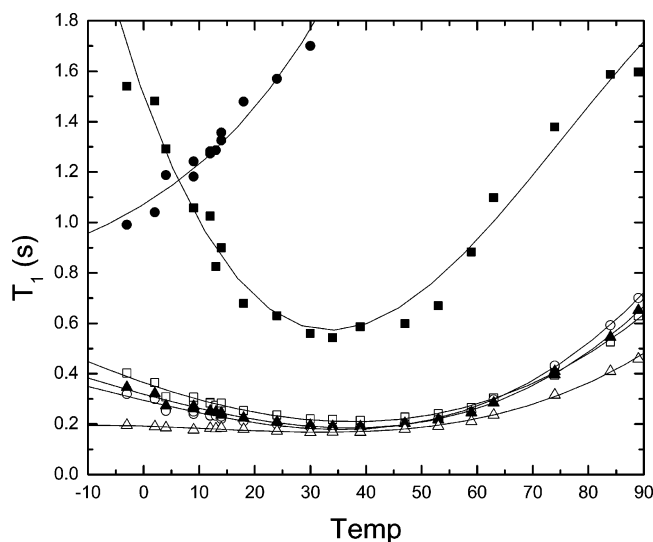


Figure 3. ^{13}C total spin lattice relaxation times (s) for [MNIM]PF₆ ionic liquid vs temperature. Imidazolium ring ^{13}C 's: 137 (□), 124 (○), and 122 ppm (▲). Ring methyl ^{13}C : 36 ppm (△). Ring methylene ^{13}C : 50 ppm (■). Nonyl terminal methyl ^{13}C : 14 ppm (●).

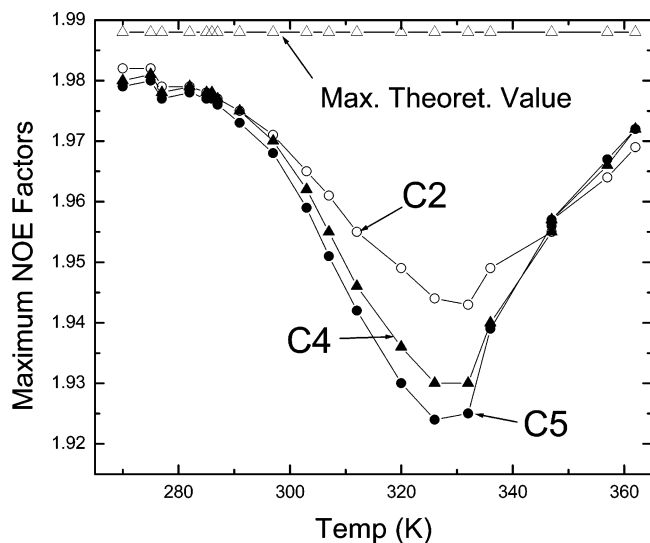


Figure 4. Corrected maximum ^{13}C NOE factors and total spin–lattice relaxation times (T_1 's) for [MNIM]PF₆ ionic liquid vs temperature: (○) imidazolium ring C2 carbon; (▲) imidazolium ring C4 and (●) C5 carbons; and (△) theoretical NOE ^{13}C maximum of 1.988.

minimal as shown in Figure 4. Although CSA effects appear for the ring methyl and adjacent methylene carbons, neither require a correction to the maximum noe factor.

Correlation Times. The corrected rotational correlation times (ns) for the imidazolium ring carbons of the [MNIM]PF₆ ionic liquid vs temperature are given in Figure 5. The initial rotational correlation times are determined by using eqs 1 (assuming complete dipolar relaxation) 7, 8, and 6 as outlined in the previous section. The corrected (final) rotational correlation times are longer (numerically greater) than the initial rotational correlation times, as the total relaxation rate is now separated into both dipolar relaxation and a second contribution (chemical shift anisotropy). The correlation time maxima observed in Figure 5 are typical for ^{13}C relaxation rate studies of ionic liquids.¹⁵ The ring and immediately adjacent carbons have correlation time maxima at higher temperatures than the remaining aliphatic carbons in the nonyl side chain.^{10–12,14,15}

The correlation time maxima of the imidazolium ring carbons (C2, C4, C5) and the methylene carbon immediately

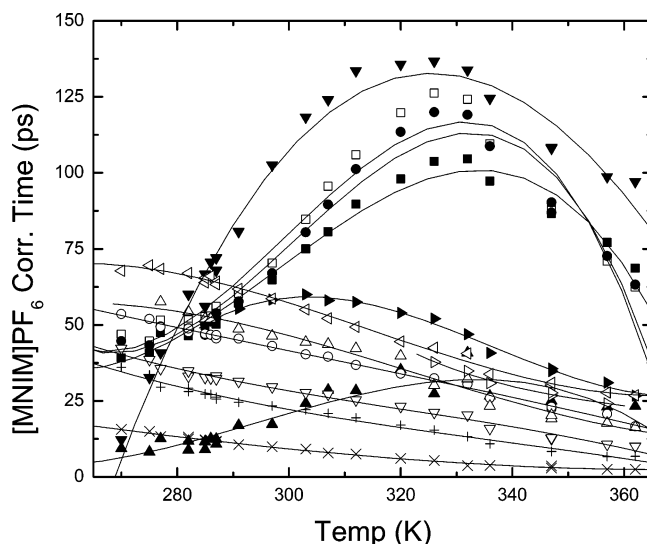


Figure 5. ^{13}C correlation times (ps) for [MNIM]PF₆ ionic liquid vs temperature. Imidazolium ring ^{13}C 's (C2, C4, C5): 137 (■), 124 (□), and 122 ppm (●). Ring methyl ^{13}C (C6): 36 ppm (▲). Ring methylene ^{13}C (C7): 50 ppm (▼). Nonyl terminal methyl ^{13}C (C15): 14 ppm (×). Additional nonyl methylene ^{13}C 's include the following: C13, 32 ppm (▽); C11, 30.2 ppm (right pointing solid triangle); C12, 29.7 ppm (○); C10, 29.4 ppm (△); C9, 29.3 ppm (right pointing open triangle); C8, 26.5 ppm (left pointing open triangle); and C14, 23 ppm (+).

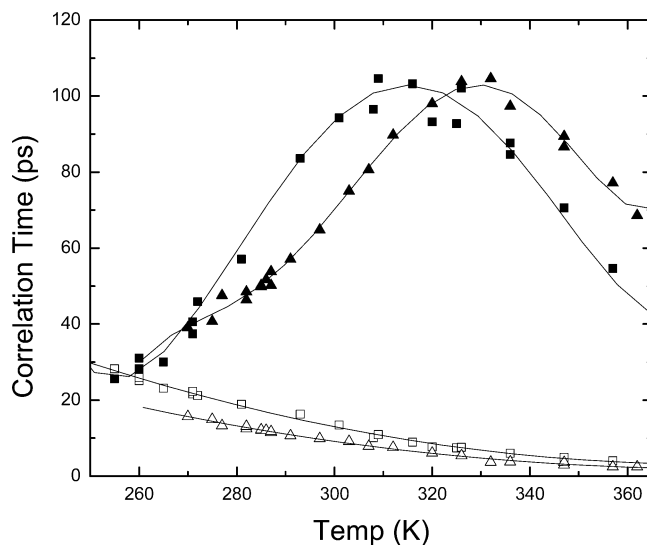


Figure 6. ^{13}C correlation times (ps) for [BMIM]PF₆ and [MNIM]PF₆ ionic liquids vs temperature: imidazolium ring ^{13}C 's (C2) for [BMIM]PF₆ (■) and [MNIM]PF₆ (▲) and terminal methyl C's for [BMIM]PF₆ (□) and [MNIM]PF₆ (△).

adjacent to the imidazolium ring (C7) are at similar temperatures, indicating ring rotation at a similar rate. The imidazolium ring methyl carbon (C6) correlation time reaches a maximum at a lower temperature as do the remaining carbons in the nonyl side chain (C8 thru C15). These results are consistent with the nonyl side chain being able to move more freely than the imidazolium ring, as one would expect.

Figure 6 compares ^{13}C correlation times (τ_c) vs temperature for [BMIM]PF₆ and [MNIM]PF₆ ionic liquids. The correlation time (τ_c) maximum for the imidazolium ring C2 carbon in [BMIM]PF₆ is located at a lower temperature (≈ 310 K) than in the more viscous [MNIM]PF₆ (≈ 325 K). The side chain terminal carbons exhibit monotonic increasing τ_c values with decreasing temperature. At high temperatures, the side chain

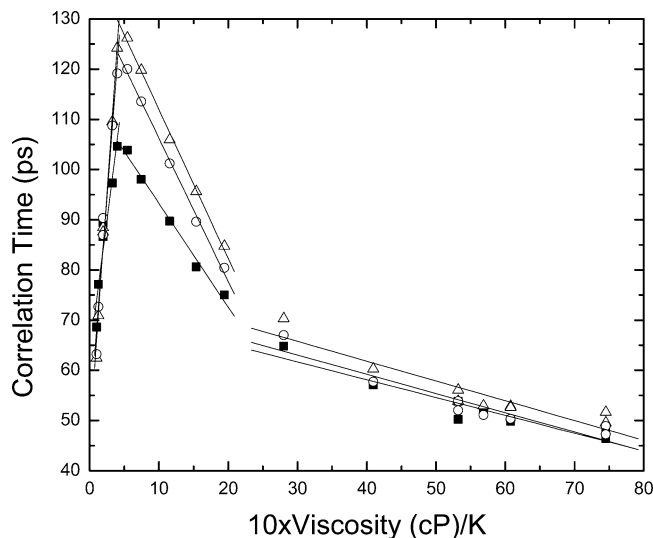


Figure 7. Correlation time (ps) for C2 (■), C4 (○), and C5 (△) vs viscosity/K (cP/K) for [MNIM] in [MNIM]PF₆. From left to right, temperature ranges include 362–332, 326–303, and 297–282 K.

(butyl and nonyl) terminal carbon τ_c values approach each other as one might expect.

NMR Correlation Times and Viscosity. In classical mechanics, the correlation time, τ_c , of a spherical particle undergoing isotropic rotation is given by the SED equation:

$$\tau_c = 4\pi a^3 \eta / 3kT = V\eta/kT \quad (10)$$

For those correlation times determined by NMR, the relationship between τ_c and temperature in the viscosity-dependent region is given by eq 11:²¹

$$\tau_c = \tau_o + \eta\tau_{\text{red}}/T \quad (11)$$

where $\tau_{\text{red}} = V/k$. The values of a , the hydrodynamic radius, obtained from this type of analysis are typically too small^{22–26} and are often corrected by using a nonspherical rotational model.²¹

Figure 7 contains a plot of NMR correlation times vs viscosity for the [MNIM]PF₆ ionic liquid. The viscosity data were obtained by extrapolation from [MNIM]PF₆ viscosity data published elsewhere.²⁷ It would appear from Figure 7 that [MNIM]PF₆ undergoes several phase changes and the only region where the slope is positive is at the higher temperatures between 59 and 89 °C. The slope in this temperature range is 632 ps-K/cP that translates into a value of 1.28 Å for the 1-methyl-3-nonylimidazolium cation. This may be compared with an a value of 1.15 Å obtained for the 1-ethyl-3-methylimidazolium cation in a 1-ethyl-3-methylimidazolium chloride–ethyl aluminum chloride melt.¹² The values of 1.28 and 1.15 Å are unrealistic and can be corrected to more reasonable values by using “frictional” correction factors.

The classical model of a sphere rotating in a continuous medium may be adjusted to account for the results obtained from eq 10 by using either the Gierer–Wirtz²⁸ or Hu–Zwanzig²⁹ models. The Gierer–Wirtz model²⁸ introduces a rotational microviscosity factor f whose radius ratio dependence is given by:

$$f = [6(a_s/a) + (1 + a_s/a)^{-3}]^{-1} \quad (12)$$

where a_s = the solvent radius and the functional dependence of f upon a_s/a results in only a minor correction when the solvent

molecule is very small or the solute molecule is very large. For neat and other liquids where the solute and solvent sizes are similar, f is 0.16. In cases where the solvent molecule is very large compared to the solute (10:1), f may be as small as 0.02.

The Gierer–Wirtz model is an adjustment for spherical molecules that corrects for the observation that molecular rotational friction coefficients are less than the Stokes value of $8\pi\eta a^3$. The Gierer–Wirtz model is adequate for describing rotation about the symmetry axis; however, rotation of the symmetry axis requires displacement of solvent molecules.

As indicated previously, the classical “stick” (SED) frictional model does not accurately represent the [MNIM]PF₆ ionic liquid as evidenced by the unrealistic a value of 1.28 Å for the 1-methyl-3-nonylimidazolium cation. The calculated gas-phase volumes of the 1-methyl-3-nonylimidazolium cation and the PF₆ anion (Figure 1) are approximately 300 and 100 Å³, respectively. The calculated gas-phase value of a for the 1-methyl-3-nonylimidazolium cation is 4.15 Å that would require a correction factor (f) of 0.029. The calculated gas-phase value of a for the PF₆ anion is 2.88 Å, resulting in an a_s/a ratio of 0.69 and a correction factor (f) of 0.23. This results in an increase (correction) of the cation a value from 1.28 to 2.09 Å or approximately one-half of the expected value (4.15 Å).

Alternatively, ionic liquids are seldom spherical and often may be regarded as prolate (cigar-shaped: $a = b < c$) or oblate (pancake-shaped: $a < b = c$) spheroids whose rotational motion is anisotropic.^{21,29} The Hu–Zwanzig²⁹ slipping boundary model accounts for the viscous drag frictional coefficient in both the prolate and oblate spheroid models over a range of a/c values. In view of the nonyl side chain in the [MNIM]PF₆ ionic liquid (Figure 1), it seems reasonable to assume that the [MNIM] cation may be considered as a prolate spheroid undergoing anisotropic rotational motion. One can only estimate a , b , and c axis values for the [MNIM] cation. The distance from the methyl group to the end of the nonyl side chain can be estimated at approximately 24 ± 2 Å. The other axes are estimated at 3 ± 1 Å. These estimated values result in a f_{slip} correction factor of 0.11 that is an improvement over the correction factor of 0.23 obtained from the Gierer–Wirtz²⁸ model. This translates to a corrected spherical (SED) a value of 2.67 Å or 64% of the theoretical gas-phase a value (4.15 Å) and is satisfactory, considering the various approximations used herein.

In addition to the analysis of the [MNIM] cation, the previously reported ¹³C NMR relaxation results of the [BMIM]PF₆ ionic liquid^{15,16} are combined with recent viscosity data²⁷ and gas-phase calculations¹⁷ to estimate the size of the [BMIM] cation. Figure 8 is a plot of [BMIM]PF₆ imidazolium ring carbon correlation times (τ_c) as a function of viscosity and temperature. As is the case with the [MNIM]PF₆ ionic liquid (Figure 7), a linear segment is located at high temperatures (326–357 K) and there appear to be several phase changes over the entire temperature range (255–357 K). The slopes of the imidazolium ring carbon (C2, C4, C5) correlation times vs $10 \times$ viscosity/K are 415, 462, and 451 ps-K/cP that convert to a values (eq 10) of 1.11, 1.15, and 1.14 Å, respectively. These values for the [BMIM] cation are considerably smaller than the a value of 3.60 Å obtained from a gas-phase calculation.¹⁷ Using the gas phase¹⁷ a value of 2.88 Å for the PF₆ anion, one obtains a a_s/a ratio of 0.80 and a correction factor (f) of 0.20 for the Gierer–Wirtz spherical model (eq 12). This correction factor increases the [BMIM] a value from an average a value of 1.13 Å to 1.93 Å that is 54% of the theoretical gas-phase value of 3.60 Å.

The distance from the methyl group to the end of the butyl side chain in the [BMIM] cation can be estimated at ap-

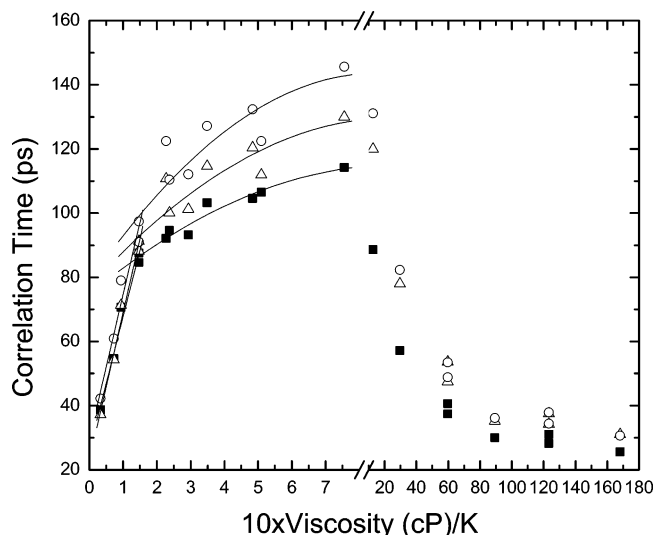


Figure 8. Correlation time (ps) for C2 (■), C4 (○), and C5 (△) vs viscosity/K (cP/K) for [BMIM] in [BMIM]PF₆. From left to right, temperature ranges include 357–326, 326–301, and 301–255 K.

proximately 12 ± 2 Å and the other axes are estimated at 3 ± 1 Å.¹⁷ These estimated gas-phase axes result in a prolate (cigar shaped) Hu–Zwanzig²⁹ f_{slip} correction factor of 0.12 that is an improvement over the correction factor of 0.20 obtained from the Gierer–Wirtz²⁸ model. This results in a corrected spherical (SED) a value of 2.29 Å or 64% of the theoretical gas-phase a value (3.60 Å).

Chemical Shift Anisotropy (CSA). The chemical shift anisotropy (eq 5) is typically defined as:

$$\Delta\sigma = |\sigma_{\parallel} - \sigma_{\perp}| = \sigma_{zz} - (\sigma_{xx} + \sigma_{yy})/2 \quad (13)$$

with $|\sigma_{zz}| \geq |\sigma_{yy}| \geq |\sigma_{xx}|$. The asymmetry parameter, η_{csa} , is generally ignored (as mentioned previously) in chemical shift anisotropy analysis as it would normally result in less than a 5–10% correction as shown in solid state¹⁹ isotropic studies. With use of the convention outlined for eq 9, the asymmetry factor is given by:^{1–6,30}

$$\eta_{\text{csa}} = (3/2)(\sigma_{xx} - \sigma_{yy})/\Delta\sigma \quad (14)$$

Figure 9 contains a plot of ^{13}C CSA vs temperature for the [MNIM]PF₆ ionic liquid. CSA is observed for the imidazolium carbons and those carbons immediately adjacent to the ring. The remaining aliphatic carbons exhibit only dipolar relaxation as expected. The chemical shift anisotropy, $\Delta\sigma$, is similar for ring carbons and the methyl carbon over the temperature range 270–362 K. However, the methylene carbon immediately adjacent to the imidazolium ring undergoes a continual increase in CSA with decreasing temperature (temperatures lower than 270 K produced ^{13}C relaxation data that could not be analyzed). Maximum values of $\Delta\sigma$ for [MNIM]PF₆ are reached at 285 K, compared with a maximum of 293 K for the [BMIM]PF₆ ionic liquid.¹⁶

The $\Delta\sigma$ values for the ring C2, C4, and C5 carbons reach maximum values of 154, 170, and 168 ppm at 285 K and then decrease to lower values at both higher and lower temperatures. The averaged $\Delta\sigma$ values for C2, C4, and C5 over the entire temperature range are 120, 129, and 126 ppm. The maximum $\Delta\sigma$ values for the three imidazolium ring carbons (154, 170, and 166 ppm) may be compared with isotropic values of 159 and 157 ppm for pyrimidine in liquid crystal solutions.³¹ There is still the unresolved question of temperature dependence.¹⁶

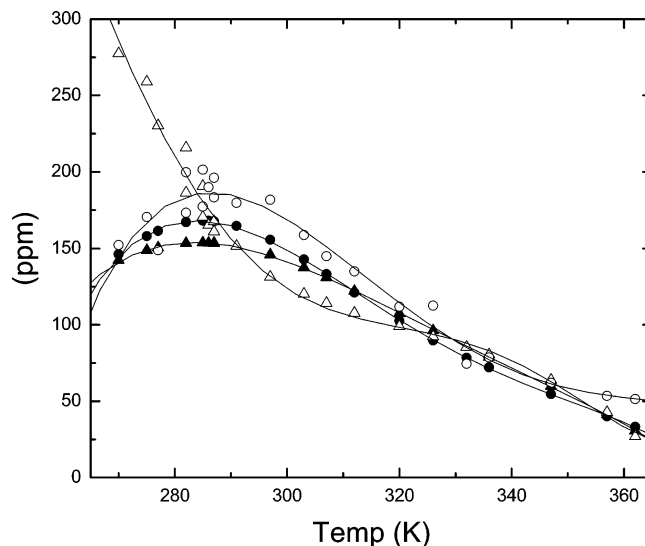


Figure 9. ^{13}C $\Delta\sigma$ (ppm) for [BMIM][PF₆] ionic liquid vs temperature: (▲) imidazolium ring C2 carbon; (●) average of imidazolium ring C4 and C5 carbons, (○) C6 methyl carbon, and (△) C7 methylene carbon.

A possible explanation is that this is merely a manifestation of changing dynamics. Alternatively, [BMIM]PF₆ and [MNIM]PF₆ ionic liquids are systems of ion pairs that have considerable equilibrium characteristics. Even in static systems, relatively small changes in the position of a single hydrogen atom can result in major shifts in the tensorial shieldings.³² It has also been reported that the isotropic average of the shielding tensor is closely related to the isotropic shift in liquids, showing only little dependence on packing in the solid state.³⁰ In view of these observations, perhaps the temperature dependence of $\Delta\sigma$ in [BMIM]PF₆ and [MNIM]PF₆ ionic liquids is to be expected.

Acknowledgment. Financial support by the Deutsche Forschungsgemeinschaft (Merkator Visiting Professorship for W.R.C.) is gratefully acknowledged. The authors also thank Prof. M. D. Zeidler for his support of this work.

References and Notes

- (1) Abragam, A. *Principles of Nuclear Magnetism*; Oxford University Press: Oxford, U.K., 1961; Chapter 8.
- (2) Farrar, T. C.; Becker, E. D. *Pulse and Fourier Transform NMR. Introduction to Theory and Methods*; Academic Press: New York, 1971.
- (3) Spiess, H. W. In *NMR: Basic Principles and Progress*; Diehl, P., Fluck, E., Kosfeld, R., Eds.; Springer-Verlag: Berlin, Germany, 1978; Vol. 15, p 55.
- (4) Canet, D.; Robert, J. B. In *NMR: Basic Principles and Progress*; Diehl, P., Fluck, E., Gunther, H., Kosfeld, R., Seelig, J., Eds.; Springer-Verlag: Berlin, Germany, 1990; Vol. 25, p 46.
- (5) McConnell, J. *Nuclear Magnetic Relaxation in Liquids*; Cambridge University Press: Cambridge, U.K., 1987.
- (6) Canet, D. *Nuclear Magnetic Resonance: Concepts and Methods*; John Wiley & Sons: New York, 1996.
- (7) Halle, B.; Wennerstrom, H. *J. Magn. Reson.* **1981**, *44*, 89.
- (8) Carper, W. R. *Concepts Magn. Reson.* **1999**, *11*, 51.
- (9) Keller, C. E.; Carper, W. R. *J. Magn. Reson.* **1994**, *A110*, 125.
- (10) Larive, C. K.; Lin, M.; Piersma, B. J.; Carper, W. R. *J. Phys. Chem.* **1995**, *99*, 12409–12412.
- (11) Carper, W. R.; Mains, G. J.; Piersma, B. J.; Mansfield, S. L.; Larive, C. K. *J. Phys. Chem.* **1996**, *100*, 4724–4728.
- (12) Larive, C. K.; Lin, M.; Kinnear, B. S.; Piersma, B. J.; Keller, C. E.; Carper, W. R. *J. Phys. Chem.* **1998**, *102B*, 1717.
- (13) Neuhaus, D.; Williamson, M. P. *The Nuclear Overhauser Effect in Structural and Conformational Analysis*; Wiley-VCH Press: New York, 2000.
- (14) Dölle, A. *J. Phys. Chem. A* **2002**, *106*, 11683.
- (15) Antony, J. H.; Mertens, D.; Dölle, A.; Wasserscheid, P.; Carper, W. R. *ChemPhysChem* **2003**, *4*, 588.

- (16) Carper, W. R.; Wahlbeck, P. G.; Dolle, A. *J. Phys. Chem. A* **2004**, *108*, 6096–6099.
- (17) Meng, Z.; Dölle, A.; Carper, W. R. *J. Mol. Struct. (THEOCHEM)* **2002**, *585*, 119.
- (18) Fuller, J.; Carlin, R. T.; de Long, H. C.; Hawort, D. *Chem. Commun.* **1994**, 299–300.
- (19) Antony, J. H.; Mertens, D.; Breitenstein, T.; Dölle, A.; Wasserschheid, P.; Carper, W. R. *Pure Appl. Chem.* **2004**, *4*, 255.
- (20) Werbelow, L. *J. Am. Chem. Soc.* **1974**, *96*, 4747.
- (21) Boere, R. T.; Kidd, R. G. In *Annual Reports on NMR Spectroscopy*; Webb, G. A., Ed.; Academic Press: New York, 1982; Vol. 13, p 319.
- (22) Mitchell, R. W.; Eisner, J. *J. Chem. Phys.* **1960**, *33*, 86.
- (23) Mitchell, R. W.; Eisner, J. *J. Chem. Phys.* **1961**, *34*, 651.
- (24) Waylischen, R. E.; Pettitt, B. A.; Danchura, W. *Can J. Chem.* **1977**, *55*, 3602.
- (25) Kivelson, D.; Kivelson, M. G.; Oppenheim, I. *J. Chem. Phys.* **1970**, *52*, 1810.
- (26) Tyrrell, H. J. V.; Harris, K. R. *Diffusion in Liquids*; Butterworth: London, U.K., 1984.
- (27) Seddon, K. R.; Stark, A.; Torres, M. J. In *Clean Solvents: Alternative Media for Chemical Reactions and Processing*; Abraham, M. A., Moeans, L., Eds.; ACS Symp. Ser. No. 819; American Chemical Society: Washington, DC, 2002; p 34.
- (28) Gierer, A.; Wirtz, K. *Z. Naturforsch.* **1953**, *8A*, 522–532.
- (29) Hu, C. M.; Zwanzig, R. *J. Chem. Phys.* **1974**, *60*, 4354–4357.
- (30) Mehring, M. In *High-Resolution NMR Spectroscopy in Solids*; Diehl, P., Fluck, E., Kosfeld, R., Eds.; Springer-Verlag: Berlin-Heidelberg-New York; NMR—Basic Principles and Progress, 1976; Vol. 11, p 167.
- (31) Parhami, P.; Fung, B. M. *J. Am. Chem. Soc.* **1985**, *107*, 7304.
- (32) Beeler, A. J.; Orendt, A. M.; Grant, D. M.; Cutts, P. W.; Milchl, J.; Zilm, K. W.; Downing, J. W.; Facelli, J. C.; Schindler, M. S.; Kutzelnigg, W. *J. Am. Chem. Soc.* **1984**, *106*, 7672.